Title:

R406, an Orally Available Syk Kinase Inhibitor Blocks Fc Receptor Signaling and Reduces Immune Complex-Mediated Inflammation

Authors:

Sylvia Braselmann, Vanessa Taylor, Haoran Zhao, Su Wang, Catherine Sylvain, Muhammad Balloum, Kunbin Qu, Ellen Herlaar, Angela Lau, Chi Young, Brian R. Wong, Scott Lovell, Thomas Sun, Gary Park, Ankush Argade, Stipo Jurcevic, Polly Pine, Rajinder Singh, Elliott B. Grossbard, Donald G. Payan, and Esteban S. Masuda

Laboratory:

Rigel Pharmaceuticals, 1180 Veterans Blvd, South San Francisco, CA 94080, USA (SB, VT, HZ, SW, CS, MB, KQ, EH, AL, CY, BW, TS, GP, AA, PP, RS, EG, DP, EM)

deCODE Biostructures, 2501 Davey Road, Woodridge, IL 60517, USA (SL)

King's College London, Department of Nephrology and Transplantation, Guy's Hospital, London SE1 9RT, UK (SJ)

A) Running Title: Syk Inhibitor R406 blocks Fc Receptor signaling

B) Corresponding Author: Esteban S. Masuda, Rigel Pharmaceuticals, 1180 Veterans Blvd,

South San Francisco, CA 94080, USA, Tel: (650) 624-1151, Fax: (650) 624-1101, E-mail:

emasuda@rigel.com

C) Manuscript Information:

Number of text pages:	24
Number of tables:	2
Number of figures:	5
Number of references:	39
Total words in the abstract:	250
Total words in the introduction:	554
Total words in the discussion:	1500

D) List of Nonstandard abbreviations: Ig, Immunoglobulin; FcR, receptor for Fc portion of immunoglobulins; FcεRI, high-affinity type-I receptor for IgE; LPS, lipopolysaccharide; LTC4, Leukotriene C4; IL, Interleukin; TNF, tumor necrosis factor; GM-CSF, granulocyte-macrophage colony-stimulating factor; CHMC, cultured human mast cells; Syk, spleen tyrosine kinase; LAT, linker for activation of T cells; PLC, phospholipase C; PKB, protein kinase B; JNK, c-Jun N-terminal kinase; ERK, extra cellular signal-regulated kinase; BLNK, B cell linker protein; Flt3, Fms-like tyrosine Kinase 3; Zap70, Zeta-chain-associated protein kinase; Stat, signal transducers and activators of transcription; ITAM, immunoreceptor tyrosine-based activation motifs; EC_{50}, effective concentration for 50% inhibition; RA, rheumatoid arthritis; CIA, collagen induced arthritis; CAIA, collagen antibody induced arthritis; IC, immune complex

E) Recommended Section: Inflammation and Immunopharmacology

ABSTRACT

Recent compelling evidence has lead to renewed interest in the role of antibodies and immune complexes in the pathogenesis of several autoimmune disorders, such as rheumatoid arthritis. These immune-complexes, consisting of autoantibodies to self-antigens, can mediate inflammatory responses largely through binding and activating the immunoglobulin Fc receptors (FcRs). Using cell-based structure activity relationships with cultured human mast cells, we have identified the small molecule R406 as a potent inhibitor of IgE- and IgG-mediated activation of Fc receptor signaling (EC_{50} for degranulation = 56-64 nM). Here we show that the primary target for R406 is the spleen tyrosine kinase (Syk), which plays a key role in the signaling of activating Fc receptors and the B cell receptor (BCR). R406 inhibited phosphorylation of Syk substrate LAT in mast cells and BLNK/SLP65 in B cells. R406 bound to the ATP binding pocket of Syk and inhibited its kinase activity as an ATP-competitive inhibitor (Ki = 30 nM). Furthermore, R406 blocked Syk-dependent FcR-mediated activation of monocytes/macrophages and neutrophils, and BCR-mediated activation of B lymphocytes. R406 was selective as assessed using a large panel of Syk-independent cell-based assays representing both specific and general signaling pathways. Consistent with Syk inhibition, oral administration of R406 to mice reduced immune complex-mediated inflammation in a reverse passive Arthus reaction and two antibody-induced arthritis models. Finally, we report a first-in-human study showing that R406 is orally bioavailable, achieving exposures capable of inhibiting Syk-dependent IgE-mediated basophil activation. Collectively, the results show R406 potential for modulating Syk activity in human disease.

Rheumatoid arthritis (RA) is a chronic inflammatory disease of peripheral joints characterized by autoantibody expression, synovial inflammation, pannus formation, and erosions of cartilage and bone (Firestein, 2003). Despite significant efforts and advances, the etiology of RA and its pathogenesis remain incompletely understood and the available medical treatments have limited efficacy. Thus, additional therapies with tolerable side effects are desired (Firestein, 2003; Smolen and Steiner, 2003).

Current opinion purports that in genetically susceptible patients, joint inflammation in RA is triggered by the activation of innate immunity with infectious or environmental products, and perpetuated with self-sustaining autoimmune responses. RA has been associated with several types of autoantibodies directed against antigens such as type II collagen, heat-shock proteins, BiP, hnRNP-33, and citrullinated proteins, as well as with rheumatoid factors that recognize the Fc fragment of immunoglobulin G (IgG) (Steiner and Smolen, 2002). Thus, in this context, locally produced specific autoantibodies and immune complexes (ICs) can activate sentinel and effector cells leading to inflammatory mediator release and cytokine production promoting further deleterious responses resulting in synovitis and joint structural damage.

The role for ICs in RA has been bolstered by the fact that in mice, joint arthritic pathology can be elicited with the passive transfer of antibodies directed against glucose-6-phosphate isomerase (GPI) in the K/BxN model, or against collagen type II in the collagen-antibody-induced arthritis (CAIA) model (Terato et al., 1992; Ji et al., 2002; Firestein and Corr, 2005). These antibodies and their ICs engage and activate Fc receptor (FcR) signaling in macrophages, neutrophils, dendritic and mast cells resulting in degranulation and cytokine gene transcription, which is critical for disease initiation and propagation. Importantly, synovial and articular inflammation induced by these antibodies was markedly suppressed in mice deficient in the FcRγ

gene, the signaling component of activating Fcγ receptor complexes (Ji et al., 2002; Kagari et al., 2003). Thus, blocking this FcR signaling represents an attractive strategy for therapeutic intervention of IC-mediated inflammation.

FcRγ signal transduction is critically dependent on immunoreceptor tyrosine-based activation motifs (ITAMs) located in its cytoplasmic tail (Berton et al., 2005; Nimmerjahn and Ravetch, 2006). Spleen Tyrosine Kinase (Syk), expressed predominantly in haematopoietic cells, binds these phosphorylated ITAM motifs and activates the events needed for downstream signaling. Syk is also essential for signal transduction of ITAMs which are present among others in the B cell receptor, the NK cell DAP12 receptor, and the platelet Glycoprotein VI receptor (Turner et al., 2000; Wong et al., 2004; Berton et al., 2005). Syk is thus a central player in the activation of immune cells likely playing critical roles in the pathogenesis in RA.

Here we describe the identification and biological characterization of R406 as a small molecule inhibitor that primarily targets Syk. We show that R406 is orally available and potently inhibits IgE- and IgG-mediated activation of Fc receptor signaling. R406 inhibits the ITAM-dependent signaling by the Fc receptor complexes in macrophages, neutrophils and mast cells, and the ITAM-dependent signaling from the B-cell receptor. In mice, administration of R406 reduced vascular leakage and edema in the Arthus reaction elicited by immune complexes. R406 also showed efficacy in inhibiting paw inflammation in two antibody-induced arthritis mouse models. Finally, we report a first-in-human study with R406, in which in addition to preliminary observations on safety and pharmacokinetics, we assessed the effects of R406 on basophil activation and platelet aggregation.

METHODS

R406

The small molecule N4-(2,2-dimethyl-3-oxo-4H-pyrid[1,4]oxazin-6-yl)-5-fluoro-N2-(3,4,5-trimethoxyphenyl)-2,4-pyrimidinediamine (R406) was synthesized by the Department of Chemistry of Rigel Pharmaceuticals, Inc. The structure of R406 is shown in Figure 1e. The discovery and structure-activity relationship leading to R406 will be presented elsewhere (R. Singh, manuscript in preparation).

Human Mast Cell (CHMC) Culture and Stimulation

Cultured human mast cells (CHMC) were derived from cord blood CD34+ progenitor cells, and grown, primed and stimulated as described previously [Rossi et al., in press] and in the **Supplementary Methods** online. Prior to stimulation, cells were incubated with R406 or DMSO for 30 min. Cells were then stimulated with either 0.25-2 mg/mL anti-IgE or anti-IgG (Bethyl Laboratories), or 2 µM ionomycin (VWR International). For tryptase measurement, ~1,500 cells per well were stimulated for 30 minutes in MT buffer. For LTC_4 and cytokine production, 100,000 cells per well were stimulated for 1 hour or for 7 hours, respectively. Tryptase activity was measured by luminescence readout of a peptide substrate, and LTC_4 and cytokines were measured using Luminex multiplex technology.

Western Blot

Cells were pre-incubated at $1x10^6$ cells/mL with DMSO vehicle or R406 at different concentrations for 40 minutes, and stimulated with 2 µg/mL anti-human IgE for 5 minutes, or as indicated in the figure legend. The cells were spun down, washed in PBS, and re-suspended in Tris-Glycine SDS sample buffer. For immunoprecipitations, $10x10^6$ cells/mL were stimulated as described above and precipitated according to standard protocol. Western blots were performed

6

according to standard protocol, using 8% Tris-Glycine gels, Immobilon P membrane, and ECL Western blot detection reagent. Primary antibodies were purchased from Cell Signaling Technologies. Membranes were re-probed with antibodies recognizing various other proteins to verify equal amount of protein in each lane.

In-vitro Fluorescence Polarization (FP) Kinase Assay and Ki Determination

The FP reactions were performed as described elsewhere (see **Supplementary Methods** online). For K_i determination, duplicate 200 µL reactions were set up at eight different ATP concentrations from 200 µM (2-fold serial dilutions) either in the presence of DMSO or R406 at 125 nM, 62.5 nM, 31.25 nM, 15.5 nM or 7.8 nM. At different time-points, 20 µL of each reaction was removed and quenched to stop the reaction. For each concentration of R406, the rate of reaction at each concentration of ATP was determined and plotted against the ATP concentration to determine the apparent K_m and V_{max} (maximal rate). Finally the apparent K_m (or apparent K_m/V_{max}) was plotted against the inhibitor concentration to determine the K_i. All data analysis was performed using Prism and Prism enzyme kinetics programs.

Crystallography

The kinase domain of spleen tyrosine kinase (Syk) encompassing amino acid residues I358 to N635 with the single mutation E440Q was crystallized by deCode Genetics. The data from a single crystal were collected to 2.3 Å resolution in the Advanced Photon Source Structural Biology Center Beamline 19-BM at Argonne National Laboratory, using a custom built CCD detector and 1o w-scans at a wavelength of 0.97934 Å. Indexing indicated a primitive orthorhombic lattice with $a = 39.94$ Å, $b = 85.24$, $c = 91.02$ Å and the space group was determined to be $P212121$. The structure was solved by molecular replacement using MOLREP version 8.2.

Stimulation of Macrophages Derived from Primary Monocytes with IgG or LPS

Human primary macrophages were derived from CD14$^+$ PBMC (AllCells, LLC) according to the protocol specified in the Monocyte Isolation Kit (Milteny Biotec) and by subsequently expanding the monocytes in 100 ng/mL human M-CSF for five days to drive differentiation to macrophages (Munn and Cheung, 1989). THP-1 cells (ATCC) cells were primed with 10 ng/mL IFNγ for six days prior to stimulation. Monocyte-derived macrophages were stimulated by immobilized (plate-bound) human IgG (Marsh et al., 1997). R406 and 15,000 cells were added to the IgG-coated wells and incubated for 16 to 20 hours at 37°C. LPS was used at a final concentration of 10 ng/mL in uncoated wells. TNFα concentration in the supernatants was measured by Luminex assay.

Stimulation of Primary Neutrophils with IgG or PMA

Primary human neutrophils were isolated from heparinized human peripheral blood following Ficoll-Hypaque gradient separation and red blood lysis. Neutrophils were preincubated with R406 or DMSO in PBS + 0.1% BSA + 5 mM glucose for 20 min at room temperature. The cells were primed with TNFα (20 ng/mL) and stimulated for 15 minutes at 37°C with rabbit anti-human IgG (0.4 µg/mL), or phorbol 12-myristate 13-acetate (PMA, 0.1 µM). Respiratory burst activity was measured by adding dihydrorhodamine 123 (DHR123) to a final concentration of 0.5 µM and incubated for 10 minutes at 37°C. The cells were fixed and intracellular fluorescence analyzed by flow cytometry.

Stimulation of Primary B-cells with anti-IgM

Primary human B-cells were isolated from peripheral blood by Ficoll-Hypaque gradient separation, followed by positive selection using CD19-coated magnetic beads according to manufacturer's instruction (Dynal Biotech). Alternatively, purified primary B-cells were

8

obtained from AllCells, LLC. Isolated B cells (65,000/well) were preincubated for 60 minutes with R406 in RMPI 1640 + 10% FBS. Cells were stimulated with anti-IgM (5 µg/mL) for 6 hours, stained with anti-CD69APC, and analyzed by flow cytometry.

Microbicidal Activity of Neutrophils

Neutrophils purified from human peripheral blood were pretreated with R406 or DMSO for 1 hour at 4°C, then mixed with opsonized *Staphylococcus aureus* bacteria in a 1:1 ratio. The samples were rotated at 37 °C and at the indicated times aliquots were plated on to blood agar plates and cultured overnight. Colony counts relative to the 0 min time-point were used to determine the percentage of bacterial growth. The positive control, cytochalasin D, inhibits neutrophil microbicidal activity as shown by robust bacterial growth.

Animals

Female Balb/c mice (Hilltop Laboratories) age 6-8 weeks were used in the collagen antibody-induced arthritis (CAIA) studies. Female C57BL/6 mice were used in the Arthus studies and in the K/BxN model performed by Dr. Diane Mathis at the Joslin Diabetes Center, Harvard Medical School. All animals used in these studies were under protocols approved for each model by each Institutional Animal Care and Use Committee.

Arthus Reaction

Reagents were obtained from Sigma Chemical Co. Mice were challenged intravenously with 1% ovalbumin (OVA) in saline (10 mg/kg) containing 1% Evans Blue dye. Ten minutes later, mice were anesthetized with isofluorane and shaved dorsolaterally. The rabbit anti-OVA IgG (50 µg/25 µL) was injected intradermally on the left side of the back at three adjacent locations. Three injections of rabbit polyclonal IgG (50 µg/25 µL) on the opposite side of the same animal

served as controls. R406, or vehicle (67% PEG400), was administered to animals 60 minutes prior to antibody/antigen challenge. Four hours after challenge, the animals were euthanized, and skin tissue was assessed for edema and inflammation by measuring dye extravasation into the surrounding tissue. Punch biopsy of the injection sites (8 mm) were incubated in 2 mL formamide at 80°C overnight. The concentration of the extravasated Evans Blue dye was measured spectrophometrically at OD_{610}.

CAIA

Balb/c mice were passively sensitized by intravenous (IV) administration of CIA® Monoclonal Antibody Blend, (Chemicon International Inc) on day 0, followed by LPS (25 μg) administered intraperitoneally (IP) on day 2 (Terato et al., 1992; Kagari et al., 2003). Mouse IgG (IV, day 0) and LPS (IP, day 2) were administered to a separate group of mice as a negative control, as well as an untreated and non-immunized naive group. R406 was administered orally, b.i.d, for 14 days, starting 4 hours after antibody challenge on day 0. Vehicle (35% TPGS; 60% PEG400; 5% PG; TPGS) was given to control animals. For the assessment of clinical scores see **Supplementary Methods** online.

K/BxN Model

Arthritis was induced in C57BL/6 mice by intraperitoneal injection of 150 μl of pooled sera from adult K/BxN mice on days 0 and 2. R406 or vehicle (35% TPGS; 60% PEG400; 5% PG) was administered orally one hour before serum injection (Ji et al., 2002). R406 or vehicle was then administered orally b.i.d, for 13 days. Ankle thickness and arthritis were scored daily. Scores of each limb (0 no disease; 1 = subtle inflammation (metatarsal phalanges joints, individual phalanx or localized edema); 2 = easily identified swelling; 3 = swelling in all aspects of paw) were summed, with the maximum score being 12.

Clinical Study

This was a double blind, placebo-controlled, ascending single dose, randomized study in normal healthy human male volunteers, conducted at a single clinical research unit. Informed consent statements were obtained from all subjects. Subjects were admitted to the unit one day prior to dosing and discharged 48-72 hours after dosing. There were five groups of subjects with 6-8 per group (one or two control subjects per group). The dose assignments were 80, 250, 400, 500, and 600 mgs respectively. The protocol was reviewed and approved by the Institutional Research Ethics Committee for the Drug Research Unit at Guy's Hospital, London, United Kingdom. For detail on the study design see **Supplementary Methods** online.

Data Analysis

All IC_{50} and EC_{50} values in biochemical and cell based assays were determined using GraphPad Prism 3.0 software and Prism Enzyme programs (San Diego, CA). Results are presented as the average ± StDev. Statistical significance was determined using the two-tailed Student t-test. Pharmacokinetic analyses were performed utilizing a WinNonLin software package.

RESULTS

R406 specifically blocks FcεRI signaling in mast cells

IgE-mediated activation of mast cells occurs through FcεRI receptors and results in

degranulation, and the synthesis of lipid mediators and cytokines (Galli et al., 2005). To find

specific FcεRI signaling inhibitors, we screened for small molecule compounds that inhibited

degranulation of cultured human mast cells (CHMC) elicited by FcεRI crosslinking with anti-IgE

antibodies but not by the calcium ionophore ionomycin (Rossi, et al., in press). Medicinal

chemistry of initial hits using cell-based structure-activity relationships resulted in the

identification of R406. R406 dose-dependently inhibited anti-IgE mediated CHMC degranulation

measured as tryptase release ($EC_{50} = 0.056 \pm 0.02$ μM) but showed no activity on ionomycin

triggered tryptase release, indicating that R406 is specific to FcR signaling and not degranulation

per se (Fig 1a). As intended, this specific inhibition also implies that R406 site of action is

proximal to the receptor complex and upstream of calcium mobilization. Importantly, R406 also

inhibited the anti-IgE induced production and release of leukotriene LTC_4, and cytokines and

chemokines, including TNFα , IL-8 , and GM-CSF (Table 1).

Syk kinase activity is the primary target for R406

Studies to date have shown that FcεRI signaling induced by receptor crosslinking is initiated

by the sequential activation of the tyrosine kinases Lyn and Syk (Siraganian, 2003; Galli et al.,

2005). Lyn, a member of the Src kinase family, is the first kinase to be activated leading to the

phosphorylation of FcRγ chain of the FcεRI complex on its ITAM motifs, the recruitment of Syk

to the phosphorylated ITAM, and the subsequent phosphorylation of Syk on Tyrosine 352 (Law

et al., 1996). Activated Syk then directly phosphorylates the adaptor molecule LAT on Tyrosine

12

191 (Galli et al., 2005), critically contributing to the formation of signaling hubs necessary for downstream signal transduction.

Interestingly, R406 did not inhibit phosphorylation of Syk Tyrosine 352, but inhibited the phosphorylation of LAT Tyrosine 191, strongly suggesting that R406 inhibited Syk but not Lyn kinase activity (Fig 1b). Consistent with the inability of inhibiting Lyn activity, R406 also did not block the Lyn-dependent phosphorylation of the FcRγ chain (Figure 2). On the other hand, the Src family kinase inhibitor PP2 potently inhibited the Lyn-dependent phosphorylation of Syk Tyrosine 352, and the subsequent Syk-dependent phosphorylation of LAT (Fig 1b). Analogous results were obtained using murine bone-marrow derived mast cells stimulated through their FcεRI and Ramos B-cells stimulated through their B-cell receptor indicating that these results were not specific to CHMC (Figure 2). Furthermore, inhibition of Syk by R406 resulted in inhibition of all phosphorylation events downstream of Syk signaling (Siraganian, 2003; Galli et al., 2005), including the phosphorylation of PLCγ1 (Y783), Akt/PKB (S473), ERK (T202/Y204), p38 (T180/Y182) and JNK (T183/Y185) (Figure 1c). Thus, the results show that R406 selectively inhibited Syk-dependent signaling in cells.

To confirm Syk inhibition by R406 we turned to biochemical Syk kinase studies. Fittingly, R406 potently inhibited Syk kinase activity in vitro with an $IC_{50} = 41$ nM measured at an ATP concentration corresponding to its Km value. Moreover, subsequent enzyme kinetic studies showed R406 to be a competitive inhibitor for ATP binding with a Ki of 30 nM (Figure 1d). In concordance with this mode of action, diffraction data collected from crystals of human Syk protein kinase domain (I358 – N635) soaked with R406 indicated electron density consistent with R406 competing with ATP for binding to the same pocket (Figure 1f-h). Refined structures showed R406 binding the receptor in a "U" shape conformation. The N1 on the pyrimidine and

N2 on the linker secure the key contacts with the hinge region of Syk, whereas the methoxylated phenyl and hetero bicyclic ring enhance the interaction dramatically by multiple hydrogen bonds and hydrophobic interactions. A summary of crystallographic data and key interactions are shown in **Supplementary Table 1** online. Taken together, the cellular and biochemical assays clearly demonstrate R406 as an ATP-competitive inhibitor of Syk kinase activity. In addition, a comparative analysis of over a thousand R406 analogs demonstrated a close positive correlation between inhibitory activity in IgE-mediated mast cell degranulation and *in vitro* Syk kinase activity, whereas no such correlation was observed with other tested kinase activities (data not shown).

For an initial selectivity assessment, R406 was profiled at 0.3 µM against a panel of over 90 *in vitro* kinase assays using a fixed ATP concentration of 10 µM for all kinase assays. Then, those significant kinases that were substantially inhibited by R406 were further tested in cells using phospho-peptide specific antibodies for known phosphorylation targets of the respective kinases. The results indicated that in cells, R406 inhibited all other kinases tested at 5 to 100 fold less potency than Syk as judged by phosphorylation of target proteins (Figure 2). After Syk, most potently inhibited by R406 was Flt3 autophosphorylation at about 5-fold less potency than Syk activity (Figure 2).

We also assessed selectivity of FcR signaling inhibition by R406 using a large panel of different cell-based counterassays representing a number of signaling pathways. The results, summarized in Table 2, indicate that R406 is more potent on Syk-dependent signaling than on Syk-independent pathways. Next to FcεRI signaling in CHMC, R406 inhibited most potently the signaling of IL-4 and IL-2 receptors (Table 2).

14

Finally, R406 was profiled on a broad commercial panel of receptor, ion channels and unrelated enzymatic binding assays. The primary screening, performed in duplicate at 10 μM R406, resulted in three biochemical assays being significantly inhibited (> 50% inhibition). A subsequent semi-quantitative concentration response on the three targets lead to estimated IC_{50} values: Adenosine A_3 receptor ($IC_{50} = 0.081$ μM), Adenosine transporter ($IC_{50} = 1.84$ μM), and Monoamine transporter ($IC_{50} = 2.74$ μM). Further testing in an assay measuring ligand-induced GTPγS binding to the Adenosine A_3 receptor indicated that R406 exhibited antagonistic activity with an IC_{50} estimated to be 0.093 μM. Since addition of adenosine to CHMCs did not result in activation of the cells (data not shown), we do not believe that this relatively potent inhibition of the Adenosine A_3 receptor is contributing to the inhibitory effect of R406 on mast cells.

The collective cellular and biochemical data indicates that R406 inhibits Syk kinase activity but it also demonstrates some other inhibitory activities, which should be taken into account during the interpretation of toxicology and pharmacology studies.

R406 inhibits FcγR and BCR Syk-dependent signaling

Having identified Syk kinase as a primary target for R406, we assessed its effect on other Syk-dependent pathways (Table 1 and Figure 3a) (Wong et al., 2004). Interestingly, in addition to FcεRI, CHMC also expressed FcγRI (CD64) on their cell surface and thus we utilized these mast cells to test for FcγRI signaling. As expected, R406 also inhibited anti-IgG induced CHMC degranulation (Figure 3a), production of leukotriene LTC_4, and TNFα, IL-8, and GMCSF (Table 1). Analogously, R406 also potently inhibited TNFα production induced by FcγR-crosslinking in human macrophages derived from human monocytes or the monocytic cell line THP-1 (Table 1 and Figure 3a) (Turner et al., 2000). In contrast, roughly ten fold higher levels of R406 were required to inhibit TNFα production induced by lipopolysaccharide (LPS), a mainly Syk-

15

independent event (Table 2). Similarly, in human neutrophils primed with TNFα, R406 inhibited oxidative burst induced by anti-IgG (Table 1 and Figure 3a) but not when induced by the phorbol ester PMA (Table 2) (Asman et al., 1996). Thus, R406 specifically inhibited FcγR signaling in human mast cells, macrophages and neutrophils.

Syk activity also mediates signaling from the B cell receptor (BCR), which consists of a membrane anchored IgM antibody noncovalently associated with two ITAM containing proteins, Ig-α and Ig-β (Pao et al., 1998; Turner et al., 2000). In primary B-cells isolated from human peripheral blood, R406 strongly inhibited cell surface CD69 upregulation induced by BCR-cross-linking with anti-IgM (Table 1 and Figure 3a). Hence consistent with being a Syk kinase inhibitor, R406 also blocked B-cell receptor signaling in B cells.

R406 Effects on Macrophage, Neutrophil and Platelet Function

Since Syk is expressed in macrophages and neutrophils, we assessed R406 impact on general innate immune responses. For this, we tested R406 effects on leukocyte phagocytosis, oxidative burst, chemotaxis, and microbicidal activity. Notably, FcR signaling is but one pathway among many redundant systems used by monocytes, macrophages and neutrophils to respond and eliminate microbes and foreign bodies (Janeway and Medzhitov, 2002). These other responses, which include Toll-like receptors (TLRs) and complement, are not regulated by Syk and consequently, R406 is not expected to significantly affect them.

Accordingly, R406 (up to 50 µM) had negligible effects on phagocytosis of FITC-labeled opsonized bacteria (*E.coli*-FITC) by monocytes and granulocytes in heparinized whole blood (Figure 3b). Likewise, R406 did not significantly inhibit oxidative burst activity of human leukocytes induced by phagocytosis of opsonized *E.coli* (Figure 3c); nor did R406 at 10 µM negatively affect granulocyte migration towards the chemotactic peptide N-formyl-Met-Leu-Phe

16

(fMLP), while 10 µM of the positive control cytochalasin D inhibited leukocyte migration by >85%. Importantly, R406 (up to 20 µM) did not inhibit microbicidal activity by purified primary neutrophils as measured by the killing of opsonized *Staphylococcus aureus* (Figure 3d). Collectively, these results indicate that R406 does not appear to impact negatively on bacteria-induced innate immune responses.

Similarly, a multitude of redundant pathways regulate platelet activation and thrombus formation (Ruggeri, 2002). Since Syk kinase is known to play a role in platelet activation via the collagen receptor (Glycoprotein VI) and some specific integrins ($\alpha IIb\beta 3$) (Poole et al., 1997; Obergfell et al., 2002), we assessed the effect of R406 on platelet function. For this, we tested R406 effect on hemostasis in vivo by measuring the bleeding times after tail-tip amputation in mice. R406, dosed orally up to 100 mg/kg, resulting in systemic exposures up to 25 µM, did not extend bleeding time in mice, whereas aspirin at 100 mg/kg caused an 88% prolongation of bleeding time (**Supplementary Table 2** online). Thus, high systemic exposures of R406 did not negatively impact bleeding times in mice.

Effect of R406 in mouse models for IC-mediated inflammation

To test R406 effects on IC-mediated inflammation, we first investigated the ability of R406 to inhibit the reverse passive Arthus reaction (RPA) (Ravetch and Bolland, 2001). Prophylactic treatment of mice with R406 administered 1hour prior to immune complex challenge reduced the cutaneous RPA reaction by approximately 72% and 86% at 1 and 5 mg/kg, respectively, compared with the vehicle control. The net optical density (OD) reading of extravasated dye extracted after treatment with R406 at 1 or 5 mg/kg R406 was reduced from 0.14 (vehicle) to 0.04 or 0.02, respectively ($p < 0.01$). These findings correlate with the tissue area exhibiting dye

extravasation and together show that R406 can inhibit local inflammatory injury mediated by ICs (Figure 4a and b).

Since activating Fcγ receptors expressed on synovial macrophages and mast cells are important in the onset of IC-mediated arthritis, we tested R406 in two mouse models of antibody-induced arthritis. In the passive anti-Collagen type II antibody-induced arthritis (CAIA) model (Terato et al., 1992; Kagari et al., 2003), treatment of the anti-collagen antibody challenged mice with R406 reduced inflammation and swelling, and the arthritis progressed more slowly in treated animals than in vehicle controls (Figure 4d). Starting on day 4, the majority of animals in the vehicle control group showed evidence of inflammation, predominantly in the hind-paws, and signs of progressive arthritis that reached a peak on Day 7. The arthritis of hind-paws in R406 treated animals progressed slower than those of the control group and reached their disease peak on day 10.

Representative joint histopathology of study groups from mouse hind-paws at day 14 is shown in Figure 4e. In vehicle treated CAIA groups, the histopathological examination of both the right and left paws revealed a marked chronic synovitis, with thickened joints and synovial lining, pannus formation, and infiltration of neutrophils, lymphocytes, monocytes, and macrophages. In animals treated with R406, the damage of joints was markedly reduced leaving them close to normal.

Similar results were obtained in the K/BxN serum transfer mouse model (Corr and Crain, 2002; Ji et al., 2002). Transfer of serum with affinity for glucose-6-phosphate isomerase from K/BxN mice into C57BL/6 mice results in the mast cell dependent development of arthritis in the recipient mice. Treatment of injected C57BL/6 mice with 10 mg/kg R406 bid delayed the onset

and reduced the severity of clinical arthritis. Paw thickening and clinical arthritis were reduced

by approximately 50% (Figure 4c).

Thus, R406 showed efficacy in the amelioration of the Arthus reaction and in reducing

clinical symptoms in the CAIA and K/BxN models of RA. Taken together, IC-mediated

inflammation was reduced by inhibition of Fc receptor signaling with R406.

Effect of R406 on basophil activation and platelet aggregation in healthy human volunteers

To assess suitability for human studies, R406 was entered into a double blind, placebo-

controlled, ascending single dose, randomized study in normal healthy male volunteers of ages

ranging from 18 to 31 years, and body mass index (BMI) ranging from 20 to 28.

Pharmacokinetic assessment indicated that R406 was highly bioavailable. R406 plasma

concentration increased in dose proportional fashion up to 400 mgs, then reached a plateau

(Figure 5a). The maximum R406 concentration was generally reached between 1.2-1.3 hours

after dosing and the half-life was approximately 15 hours (data not shown).

To test the effects of R406 on basophil activation, heparinized blood from volunteers was

stimulated ex vivo with anti-IgE, and degranulation was measured as CD63 cell-surface

upregulation on basophils by flow cytometry (Knol et al., 1991; Ebo et al., 2002). CD63,

localized on granule membranes of resting basophils, gets exposed to the cell surface upon

degranulation, and thus can be labeled with anti-CD63 antibodies. R406 significantly inhibited

CD63 cell-surface expression in a dose dependent manner (Figure 5a). The magnitude and

duration of the effect increased as R406 plasma concentration increased, and at the higher doses

there was significant inhibition of CD63 expression for as long as 24 hours after dosing (Figure

5b). The degree of inhibition was highly correlated with plasma concentration of R406 (Figure

5c). The plasma concentration that produces a 50% reduction of basophil activation was 496±42 ng/mL, which corresponds to an EC_{50} of 1.06 µM.

We also tested the effect of R406 on platelet aggregation in platelet rich plasma prepared from the dosed volunteers. Even at the highest doses, there was no inhibition of collagen or ADP induced platelet aggregation (**Supplementary Table 3** online).

Finally, safety assessment indicated no effects on any hematologic or chemistry safety parameters. Subjects dosed at 600 mgs complained of postural dizziness (or in one case dizziness) more frequently than those dosed with vehicle or lower doses (5/6 versus 1/8 and 4/21 respectively). Peripheral blood mononuclear flow cytometry showed no significant dose or time related effect on the circulating subsets of mononuclear cells or on a marker of monocyte activation (as determined by mean fluorescense intensity of CD86 on CD14 cells). However on subsequent studies, R406 treatment tended to cause a dose-dependent reduction of circulating $CD45^+CD14^+$ mononuclear cells 4 hours after a single dose, which was reversed when measured 20 hours later (data not shown). Since this reduction occurred at doses resulting in R406 exposures well over the pharmacodynamic EC_{50} as measured by basophil degranulation, it is unclear if Syk inhibition contributed to this effect.

DISCUSSION

Several lines of evidence have brought to the forefront the importance of immune complexes (ICs), activating Fc receptor signaling, and by extension Syk, in the inflammatory response in many autoimmune diseases such as rheumatoid arthritis, systemic lupus erythematosus, and multiple sclerosis in addition to type I hypersensitivity reactions like allergic rhinitis and asthma (Takai, 2002; Wong et al., 2004; Firestein and Corr, 2005).

Using cell-based structure activity relationships with human mast cells, we identified R406 as a specific FcεRI signaling inhibitor (Figure 1a). We report here the initial characterization of R406 and show its potential for modulating Syk activity in human disease. We determined the R406 primary mode of action to be the inhibition of Syk kinase activity in cells (Figure 1c) in an ATP-competitive manner (Figure 1e-i).

Our experience shows that isolated biochemical assays often fail to faithfully mimic the "native state" kinase activity inside cells. Thus, to assess selectivity, our preferred approach is to examine kinase inhibition in their cellular context. We therefore followed an initial profiling of R406 on a panel of kinase assays with careful assessments using anti-phosphopeptide Western blots (Figure 2). In addition, we complemented this assessment using cell-based assays representing different signaling systems that are regulated by multiple kinases (Table 2).

In this way, we found R406 potently inhibited all Syk-dependent cell-based assays tested, which included activating Fc receptor signaling in human macrophages, neutrophils and mast cells and B-cell receptor signaling in human B cells (Table 1). R406 was relatively selective to Syk inhibition as assessed by inhibition of phosphorylation in cells, and with a large panel of off-target Syk-independent cell-based assays (Figure 2 and Table 2). Beyond Syk, R406 inhibited next in potency, assays dependent on Flt3, Jak, and Lck (Figure 2 and Table 2), which for

21

inflammatory processes might be considered to be desirable properties (Firestein, 2003; Smolen and Steiner, 2003). Thus, altogether the results suggest a favorable cellular profile for R406 as an anti-inflammatory agent that primarily inhibits Syk kinase activity.

The Syk expression in macrophages and neutrophils prompted us to examine whether Syk inhibition by R406 interfered with innate immune responses. Previous reports with murine Syk-deficient cells had suggested that redundant systems allow macrophages and neutrophils to respond to bacterial pathogens in the absence of Syk (Turner et al., 2000; Mocsai et al., 2003). Indeed, neutrophil/monocyte phagocytosis, chemotaxis, oxidative burst, and microbicidal responses to bacterial products or opsonized bacteria were without significant effect at high micromolar concentrations of R406 (Figure 3).

Similarly, Syk kinase is also known to play a role in platelet activation via the collagen receptor (Glycoprotein VI) and specific integrins (αIIbβ3) (Clark et al., 1994; Poole et al., 1997). However, Law et al. (Law et al., 1999) have reported normal bleeding times in mice reconstituted with Syk-deficient platelets, and notably, humans deficient in Glycoprotein VI exhibited only mild bleeding tendency and otherwise normal coagulation parameters (Moroi et al., 1989). Consistent with these results, R406 dosed orally in mice had no effect on bleeding times (**Supplementary Table 2** online). Moreover, no inhibition of platelet aggregation induced by collagen or ADP in platelet-rich plasma from the human volunteers dosed with R406 was observed (**Supplementary Table 3** online). Thus taken together, R406 faithfully phenocopies Syk-deficiency without undue deleterious effects on hemostasis or innate immune responses to pathogens.

Next, we sought to assess the effects of Syk inhibition using R406 in several animal models of immune complex (IC) mediated inflammatory processes, known to be dependent on the

activating Fcγ receptors (Hazenbos et al., 1996; Sylvestre and Ravetch, 1996; Corr and Crain, 2002; Kagari et al., 2003). Oral administration of R406 dose-dependently inhibited edema formation and hemorrhage in the reverse passive Arthus reaction (Figure 4a and b). This is likely due to R406 inhibition of IC-induced degranulation and mediator release by perivascular mast cells as well as inhibition of macrophage and Langerhans cell activation. The complete inhibition by R406 mimicked results observed with FcRγ-deficient mice (Hazenbos et al., 1996; Sylvestre and Ravetch, 1996) implying that Syk kinase activity mediates most, if not all, of the FcR-dependent inflammatory response in the Arthus reaction.

Similarly, R406 treatment ameliorated joint swelling induced in mice with arthritogenic anti-collagen type II antibodies or K/BxN serum with affinity for glucose-6-phosphate isomerase (Figure 4d to e). The reduction of paw inflammation caused by R406 was not as complete as that observed in FcRγ-deficient mice (Kagari et al., 2003). This is likely due to insufficient drug systemic exposure as R406 is rapidly metabolized in mice (**Supplementary Fig. 1** online), and thus unlikely to reproduce the totality of the lesion in the knockout model. Significantly, despite some swelling, joint histopathology assessment indicated R406 treatments resulted in marked reduction of synovitis, pannus formation, and leukocyte infiltration (Figure 4e). It is possible that the diverse beneficial effects of inhibition with R406 are due to its broad effects on the many cells populating the inflamed synovium. Syk plays a central role in IC-mediated activation of sentinel cells (mast cells and macrophages) leading to vascular leakage, cytokine production and leukocyte infiltration; in activation of dendritic cells needed for disease propagation; and in activation of effector cells (neutrophils and macrophages) and osteoclast differentiation resulting in tissue damage and bone destruction (Wong et al., 2004).

In this regard, we have recently shown that R406 treatment has significant activity in a

rodent collagen-induced arthritis model, with improvement in clinical scores, histopathology and joint radiography (Brahn E, et al *Arthritis Rheum* 2004;50:S544). In rat models of RA, treatment with R406 lead to inhibition of inflammation as measured by reduction of cytokines in the synovial fluid and cartilage oligomeric matrix protein (COMP) in the serum. Moreover, influx of inflammatory cells into the synovium was inhibited, and bone erosion was drastically reduced (Pine et al., manuscript in preparation).

Similarly, we have recently shown in murine asthma models that R406 ameliorates airway hyperresponsiveness, pulmonary eosinophilia and goblet cell hyperplasia (Matsubara et al., 2005; Matsubara et al., 2006). IgE-FcεRI signaling is intimately associated with allergic conditions and pharmacological Syk inhibition has previously been shown to result in reduction of allergic airway inflammation (Yamamoto et al., 2003; Wong et al., 2004). Notably, a Syk inhibitor delivered via nasal spray was shown to have a clinically significant effect on the symptoms of seasonal allergic rhinitis in a park environment (Meltzer et al., 2005). R406 thus has therapeutic potential for both allergic and autoimmune inflammatory disorders. The inhibition of Syk kinase and Fc receptor signaling is likely a primary mechanism for these effects; however, the impact of additional beneficial effects by inhibition of Lck, Jak and Flt3 activities is not to be ignored and remain to be investigated further. Likewise, the potential inhibition of the Adenosine A_3 receptor by R406 needs to be considered, although the physiological significance of pharmacological modulation of human Adenosine A_3 receptors remains unclear.

Interestingly, Syk kinase has been reported to play a role in TNFα signaling in selected cell types intimately involved in inflammatory processes. Indeed, Cha, et al have recently demonstrated the presence of activated Syk in the intimal lining of synovial tissue from

24

rheumatoid arthritis patients (Cha et al., 2006). Moreover, they showed that R406 inhibited cytokine and matrix metalloproteinase production from TNFα-induced RA fibroblast-like synoviocytes.

Finally, antibody and IC-mediated inflammatory diseases usually develop in two distinct but overlapping phases: an immune response to antigens and the subsequent inflammatory process (Smolen and Steiner, 2003; Firestein and Corr, 2005). We have shown here the salutary effects of R406 on inflammation. Syk kinase is also essential for BCR signaling in B cells and FcR signaling in dendritic cells (Turner et al., 2000; Sedlik et al., 2003). Thus it will be interesting to assess in the future R406 effects on humoral immune responses, including antibody production and immunoglobulin class switching.

Importantly, R406 proved to be highly bioavailable in human subjects (Figure 5a). Oral administration of R406 induced a dose-dependent inhibition of CD63 cell-surface expression in peripheral blood basophils following stimulation by anti-IgE. The magnitude of the inhibitory effect and its duration highly correlated with the plasma concentration of R406. The disparity between the cell-based EC_{50} and the *in vivo* EC_{50} may be attributable to high protein binding of R406 in human plasma (>98%). We have seen a comparable shift in EC_{50} in Syk-dependent and Syk-independent cell-based assays when human serum was added (data not shown). Notably, no remarkable adverse effects were observed at levels of R406 that inhibited basophil activation. Overall, the pharmacokinetic and pharmacodynamic data suggests that twice per day, or even once per day, dosing might be sufficient to achieve the desired biologic reduction of Syk activity in target tissues.

In summary, we have developed R406 as a potent Syk kinase inhibitor using biology-directed drug discovery. We have shown that R406 has potential for broad anti-inflammatory

properties as it inhibits several critical nodes of the inflammatory cascade without interfering

markedly with the innate immune response or hemostasis. Our results with R406 support Syk

inhibition as a novel therapeutic approach for inflammatory arthritis and other immune-mediated

inflammatory diseases.

REFERENCES

Asman B, Gustafsson A and Bergstrom K (1996) Priming of neutrophils with tumor necrosis factor-alpha measured as Fc gamma receptor-mediated respiratory burst correlates with increased complement receptor 3 membrane density. *Int J Clin Lab Res* **26**:236-239.

Berton G, Mocsai A and Lowell CA (2005) Src and Syk kinases: key regulators of phagocytic cell activation. *Trends Immunol* **26**:208-214.

Cha HS, Boyle DL, Inoue T, Schoot R, Tak PP, Pine P and Firestein GS (2006) A novel spleen tyrosine kinase inhibitor blocks c-Jun N-terminal kinase-mediated gene expression in synoviocytes. *J Pharmacol Exp Ther* **317**:571-578.

Clark EA, Shattil SJ, Ginsberg MH, Bolen J and Brugge JS (1994) Regulation of the protein tyrosine kinase pp72syk by platelet agonists and the integrin alpha IIb beta 3. *J Biol Chem* **269**:28859-28864.

Corr M and Crain B (2002) The role of FcgammaR signaling in the K/B x N serum transfer model of arthritis. *J Immunol* **169**:6604-6609.

Ebo DG, Lechkar B, Schuerwegh AJ, Bridts CH, De Clerck LS and Stevens WJ (2002) Validation of a two-color flow cytometric assay detecting in vitro basophil activation for the diagnosis of IgE-mediated natural rubber latex allergy. *Allergy* **57**:706-712.

Firestein GS (2003) Evolving concepts of rheumatoid arthritis. *Nature* **423**:356-361.

Firestein GS and Corr M (2005) Common mechanisms in immune-mediated inflammatory disease. *J Rheumatol Suppl* **73**:8-13; discussion 29-30.

Galli SJ, Kalesnikoff J, Grimbaldeston MA, Piliponsky AM, Williams CM and Tsai M (2005) Mast cells as "tunable" effector and immunoregulatory cells: recent advances. *Annu Rev Immunol* **23**:749-786.

Hazenbos WL, Gessner JE, Hofhuis FM, Kuipers H, Meyer D, Heijnen IA, Schmidt RE, Sandor M, Capel PJ, Daeron M, van de Winkel JG and Verbeek JS (1996) Impaired IgG-dependent anaphylaxis and Arthus reaction in Fc gamma RIII (CD16) deficient mice. *Immunity* **5**:181-188.

Janeway CA, Jr. and Medzhitov R (2002) Innate immune recognition. *Annu Rev Immunol* **20**:197-216.

Ji H, Ohmura K, Mahmood U, Lee DM, Hofhuis FM, Boackle SA, Takahashi K, Holers VM, Walport M, Gerard C, Ezekowitz A, Carroll MC, Brenner M, Weissleder R, Verbeek JS, Duchatelle V, Degott C, Benoist C and Mathis D (2002) Arthritis critically dependent on innate immune system players. *Immunity* **16**:157-168.

Kagari T, Tanaka D, Doi H and Shimozato T (2003) Essential role of Fc gamma receptors in anti-type II collagen antibody-induced arthritis. *J Immunol* **170**:4318-4324.

Knol EF, Mul FP, Jansen H, Calafat J and Roos D (1991) Monitoring human basophil activation via CD63 monoclonal antibody 435. *J Allergy Clin Immunol* **88**:328-338.

Law CL, Chandran KA, Sidorenko SP and Clark EA (1996) Phospholipase C-gamma1 interacts with conserved phosphotyrosyl residues in the linker region of Syk and is a substrate for Syk. *Mol Cell Biol* **16**:1305-1315.

Law DA, Nannizzi-Alaimo L, Ministri K, Hughes PE, Forsyth J, Turner M, Shattil SJ, Ginsberg MH, Tybulewicz VL and Phillips DR (1999) Genetic and pharmacological analyses of Syk function in alphaIIbbeta3 signaling in platelets. *Blood* **93**:2645-2652.

Marsh CB, Wewers MD, Tan LC and Rovin BH (1997) Fc(gamma) receptor cross-linking induces peripheral blood mononuclear cell monocyte chemoattractant protein-1 expression: role of lymphocyte Fc(gamma)RIII. *J Immunol* **158**:1078-1084.

Matsubara S, Koya T, Takeda K, Joetham A, Miyahara N, Pine P, Masuda ES, Swasey CH and Gelfand EW (2005) Syk activation in dendritic cells is essential for airway hyperresponsiveness and inflammation. *Am J Respir Cell Mol Biol*. **34**:426-433.

Matsubara S, Li G, Takeda K, Loader JE, Pine P, Masuda ES, Miyahara N, Miyahara S, Lucas JJ, Dakhama A and Gelfand EW (2006) Inhibition of spleen tyrosine kinase prevents mast cell activation and airway hyperresponsiveness. *Am J Respir Crit Care Med* **173**:56-63.

Meltzer EO, Berkowitz RB and Grossbard EB (2005) An intranasal Syk-kinase inhibitor (R112) improves the symptoms of seasonal allergic rhinitis in a park environment. *J Allergy Clin Immunol* **115**:791-796.

Mocsai A, Zhang H, Jakus Z, Kitaura J, Kawakami T and Lowell CA (2003) G-protein-coupled receptor signaling in Syk-deficient neutrophils and mast cells. *Blood* **101**:4155-4163.

Moroi M, Jung SM, Okuma M and Shinmyozu K (1989) A patient with platelets deficient in glycoprotein VI that lack both collagen-induced aggregation and adhesion. *J Clin Invest* **84**:1440-1445.

Munn DH and Cheung NK (1989) Antibody-dependent antitumor cytotoxicity by human monocytes cultured with recombinant macrophage colony-stimulating factor. Induction of efficient antibody-mediated antitumor cytotoxicity not detected by isotope release assays. *J Exp Med* **170**:511-526.

Nimmerjahn F and Ravetch JV (2006) Fcgamma receptors: old friends and new family members. *Immunity* **24**:19-28.

Obergfell A, Eto K, Mocsai A, Buensuceso C, Moores SL, Brugge JS, Lowell CA and Shattil SJ
(2002) Coordinate interactions of Csk, Src, and Syk kinases with [alpha]IIb[beta]3
initiate integrin signaling to the cytoskeleton. *J Cell Biol* **157**:265-275.

Pao LI, Famiglietti SJ and Cambier JC (1998) Asymmetrical phosphorylation and function of
immunoreceptor tyrosine-based activation motif tyrosines in B cell antigen receptor
signal transduction. *J Immunol* **160**:3305-3314.

Poole A, Gibbins JM, Turner M, van Vugt MJ, van de Winkel JG, Saito T, Tybulewicz VL and
Watson SP (1997) The Fc receptor gamma-chain and the tyrosine kinase Syk are
essential for activation of mouse platelets by collagen. *Embo J* **16**:2333-2341.

Ravetch JV and Bolland S (2001) IgG Fc receptors. *Annu Rev Immunol* **19**:275-290.

Ruggeri ZM (2002) Platelets in atherothrombosis. *Nat Med* **8**:1227-1234.

Sedlik C, Orbach D, Veron P, Schweighoffer E, Colucci F, Gamberale R, Ioan-Facsinay A,
Verbeek S, Ricciardi-Castagnoli P, Bonnerot C, Tybulewicz VL, Di Santo J and
Amigorena S (2003) A critical role for Syk protein tyrosine kinase in Fc receptor-
mediated antigen presentation and induction of dendritic cell maturation. *J Immunol*
170:846-852.

Siraganian RP (2003) Mast cell signal transduction from the high-affinity IgE receptor. *Curr
Opin Immunol* **15**:639-646.

Smolen JS and Steiner G (2003) Therapeutic strategies for rheumatoid arthritis. *Nat Rev Drug
Discov* **2**:473-488.

Steiner G and Smolen J (2002) Autoantibodies in rheumatoid arthritis and their clinical
significance. *Arthritis Res* **4 Suppl 2**:S1-5.

Sylvestre DL and Ravetch JV (1996) A dominant role for mast cell Fc receptors in the Arthus

reaction. *Immunity* **5**:387-390.

Takai T (2002) Roles of Fc receptors in autoimmunity. *Nat Rev Immunol* **2**:580-592.

Terato K, Hasty KA, Reife RA, Cremer MA, Kang AH and Stuart JM (1992) Induction of

arthritis with monoclonal antibodies to collagen. *J Immunol* **148**:2103-2108.

Turner M, Schweighoffer E, Colucci F, Di Santo JP and Tybulewicz VL (2000) Tyrosine kinase

SYK: essential functions for immunoreceptor signalling. *Immunol Today* **21**:148-154.

Wong BR, Grossbard EB, Payan DG and Masuda ES (2004) Targeting Syk as a treatment for

allergic and autoimmune disorders. *Expert Opin Investig Drugs* **13**:743-762.

Yamamoto N, Takeshita K, Shichijo M, Kokubo T, Sato M, Nakashima K, Ishimori M, Nagai H,

Li YF, Yura T and Bacon KB (2003) The orally available spleen tyrosine kinase inhibitor

2-[7-(3,4-dimethoxyphenyl)-imidazo[1,2-c]pyrimidin-5-ylamino]nicotinamide

dihydrochloride (BAY 61-3606) blocks antigen-induced airway inflammation in rodents.

J Pharmacol Exp Ther **306**:1174-1181.

FOOTNOTES

Address correspondence to:

Esteban S. Masuda, Rigel Pharmaceuticals, 1180 Veterans Blvd, South San Francisco, CA

94080, USA

Telephone: (650) 624-1151, Facsimile: (650) 624-1101, emasuda@rigel.com

LEGENDS FOR FIGURES

Figure 1: Mechanism of Action – R406 is a Syk kinase inhibitor

(**a**) Inhibition of degranulation (tryptase release) of CHMC by R406. Primed CHMC were pre-incubated with R406, stimulated with anti-human IgE or ionomycin, and tryptase measured after 30 min. (**b**) Diagram of early Syk signaling events. α,β,γ designate FcεRI complex subunits. (c) and (**d**) Western blots using phospho-specific antibodies. Primed CHMCs were pre-incubated for 40 minutes with R406, PP2, or DMSO as indicated, stimulated with anti-human IgE for 5 minutes, and lysed in SDS buffer. Blots were probed with phospho-specific antibodies as indicated. (**e**) Ki determination of R406 with recombinant Syk protein (see Supplementary Methods online) (**f**) Chemical structure of R406 (N4-(2,2-dimethyl-3-oxo-4H-pyrid[1,4]oxazin-6-yl)-5-fluoro-N2-(3,4,5-trimethoxyphenyl)-2,4-pyrimidinediamine). (**g**) Diagram of the final $2f_o\text{-}f_c$ electron density for R406 contoured at 1σ. (**h**) Diagram of the ATP-binding pocket of Syk kinase domain containing R406. Hydrogen bonds and salt-bridges are shown. (**i**) Molecular surface of the ATP-binding pocket of Syk. The bound configurations of ATP and R406 are shown.

Figure 2: R406 selectivity. Different cell lines were pre-incubated with R406, and stimulated as indicated for 5 to 10 min. Lysates were separated on SDS PAGE gels, and the western blots were probed with antibodies specific for phosphorylated kinase targets. Flt3 and the FcR γ chain were immunoprecipitated and probed with anti-phosphotyrosine antibody.

Figure 3: R406 effect on Syk-dependent pathways and leukocyte function in innate immunity.

(**a**) R406 inhibits Syk-dependent pathways: tryptase release in CHMC induced by αIgE or αIgG,

33

CD69 surface expression in primary B-cells stimulated with αIgM, TNFα production in primary neutrophils stimulated with αIgG, and TNFα production in primary monocytes stimulated with IgG. (**b**) R406 does not inhibit phagocytosis of fluorescein (FITC)-labeled opsonized bacteria by leukocytes. Heparinized whole blood was incubated with R406 for 30 min, FITC-labeled *E.coli* was added, and phagocytosis induced and measured using the Phagotest® kit, (ORPEGEN Pharma). Cytochalasin D EC$_{50}$ = 1.8 μM. R406 EC$_{50}$ = >50 μM. (**c**) R406 does not inhibit oxidative burst induced with unlabeled opsonized *E. coli* bacteria in monocytes and granulocytes. Heparinized whole blood was incubated with R406 or Cytochalasin D for 20 min, and oxidative burst was induced and measured using the Bursttest® kit, (ORPEGEN Pharma). Cytochalasin D EC$_{50}$ = 2.7 μM. R406 EC$_{50}$ = >30 μM. (**d**) R406 does not inhibit microbicidal activity, which was tested by adding opsonized *Staphylococcus aureus* cultures to purified neutrophils for the indicated length of time.

Figure 4: Effect of R406 on mouse Immune-complex mediated disease models.
(**a**) Reduction of local edema in the Arthus model. Edema was determined by the difference in the absorbance of extravasated dye from tissues injected with specific anti-OVA compared with the absorbance of tissue injected with non-specific IgG. (Statistical significance compared to vehicle (0): ** = p<0.001). (**b**) Reduction of local edema in the Arthus model as measured by the size of the edema. (Statistical significance compared to vehicle (0): * = p<0.05, ** = p<0.01, *** = p<0.001). (**c**) Arthritis clinical scores in the K/BxN model. Arthritis is induced by passive immunization on Days 0 and 2 with serum from K/BxN adult mice. (**d**) Arthritis clinical scores in the CAIA model induced by passive immunization with arthrogenic anti-collagen antibodies. (**e**) Histology of the CAIA model. Representative hind-paw sections of the ankle joint from

different treatment groups were stained with Safranin O and photographed under light microscopy.

Figure 5: Relationship between pharmacodynamic effect and plasma concentration of R406 in humans.

(**a**) Healthy human volunteers were dosed orally with single doses of R406, and 4 hours post dose plasma concentration was measured and heparinized blood was stimulated ex-vivo with αIgE. Cell surface expression of CD63 induced by αIgE stimulation was measured by flow cytometry using anti-CD63-FITC antibodies (Basotest® kit, ORPEGEN Pharma). Basophils were identified in whole blood by positive staining with a PE labeled anti-IgE antibody. Plasma concentrations of R406 were analyzed by a validated LC-MS/MS assay. The level of R406 plasma concentration (average of 6 volunteers per group; closed bar) is correlated to the percent change of CD63+ basophils in R406 treated volunteers (normalized to baseline; open bars.) (**b**) Inhibition of basophil activation at different time points after single dosing. (**c**) Correlation between plasma concentration of R406 (ng/mL) and percent change of CD63+ basophils in normal human volunteers after single dose oral administration of R406. Each circle represents a single data point normalized to pre-dose levels. The curve represents the fit of the sigmoidal E-max model to the data. Subjects who had less than 15% CD63 expression at baseline (low responders) were excluded in this graph.

Table 1. **R406 Specifically Inhibits Syk-dependent FcR and BCR Signaling.** Inhibition by R406 was tested in a variety of Syk-dependent pathways in different cells. Each assay was optimized independently and run with appropriate controls.

Cell Type	Stimulation	Signaling Pathway	Readout	EC_{50} (μM)	StDev (μM)
Mast cells, CHMC	anti-IgE	FcϵRI	Degranulation	0.056	0.02
Mast cells, CHMC	anti-IgE	FcϵRI	Leukotriene LTC$_4$	0.093	0.076
Mast cells, CHMC	anti-IgE	FcϵRI	TNF-α	0.118	0.031
Mast cells, CHMC	anti-IgE	FcϵRI	IL-8	0.140	0.016
Mast cells, CHMC	anti-IgE	FcϵRI	GMCSF	0.158	0.025
Mast cells, CHMC	anti-IgG	FcγR	Degranulation	0.064	0.016
Mast cells, CHMC	anti-IgG	FcγR36	Leukotriene LTC$_4$	0.041	0.08
Mast cells, CHMC	anti-IgG	FcγR	TNF-α	0.082	0.053
Mast cells, CHMC	anti-IgG	FcγR	IL-8	0.053	0.012
Mast cells, CHMC	anti-IgG	FcγR	GMCSF	0.056	0.014
Monocytic line, THP-1	anti-IgG	FcγR	TNF-α	0.171	0.104
Primary human macrophages	anti-IgG	FcγR	TNF-α	0.111	0.023
Primary human neutrophils	anti-IgG	FcγR	Oxidative burst	0.033	0.008
Primary human B cells	anti-IgM	BCR	CD69 upregulation	0.048	0.026

Table 2.   **Cell-based Counter Assays.** Inhibition by R406 was tested in cell-based counter assays measuring a variety of Syk independent signaling pathways. Each assay was optimized independently and run with the appropriate controls.

Cell Type	Stimulation	Receptor Type	Readout	EC$_{50}$ (μM)	StDev (μM)
Mast cells, CHMC	anti-IgE	ITAM (FcεRI)	Degranulation	0.056	0.02
Ramos B cell line	IL-4	Cytokine (IL4R)	CD23 upregulation	0.192	0.01
Primary human T cells	IL-2	Cytokine (IL2R)	Cell proliferation	0.190	0.07
Primary human T cells	αCD3/CD28	ITAM (TCR/CD28)	IL-2 production	0.448	0.09
A549 epithelial line	TNFα	Cytokine (TNFR)	CD54 upregulation	4.8	1.82
A549 epithelial line	IL-1	Cytokine (IL-1R)	CD54 upregulation	7.87	3.76
A549 epithelial line	IFNγ	Cytokine (IFNR)	CD54 upregulation	2.14	0.78
Jurkat T cell line	PMA	PKC	CD69 upregulation	>20	
Primary human neutrophils	PMA	PKC	Oxidative burst	>10	
Mast cells, CHMC	Ionomycin	Ca channels	Degranulation	>10	
Monocytic line, THP-1	LPS	TLR4	TNF-α	2.10	1.2
Primary human macrophage	LPS	TLR4	TNF-α	1.15	0.1
Huh7 hepatocyte line	serum	General cell growth	Cell proliferation	15.1	7.48
A549 epithelial line	serum	General cell growth	Cell proliferation	2.9	0.57
H1299 lung cancer line	serum	General cell growth	Cell proliferation	6.3	3.5
HeLa	Insulin	Insulin Receptor	P-AKT (ICW)	1.19	0.28
HeLa	EGF	EGF Receptor	P-EGFR (ICW)	17.46	11.57

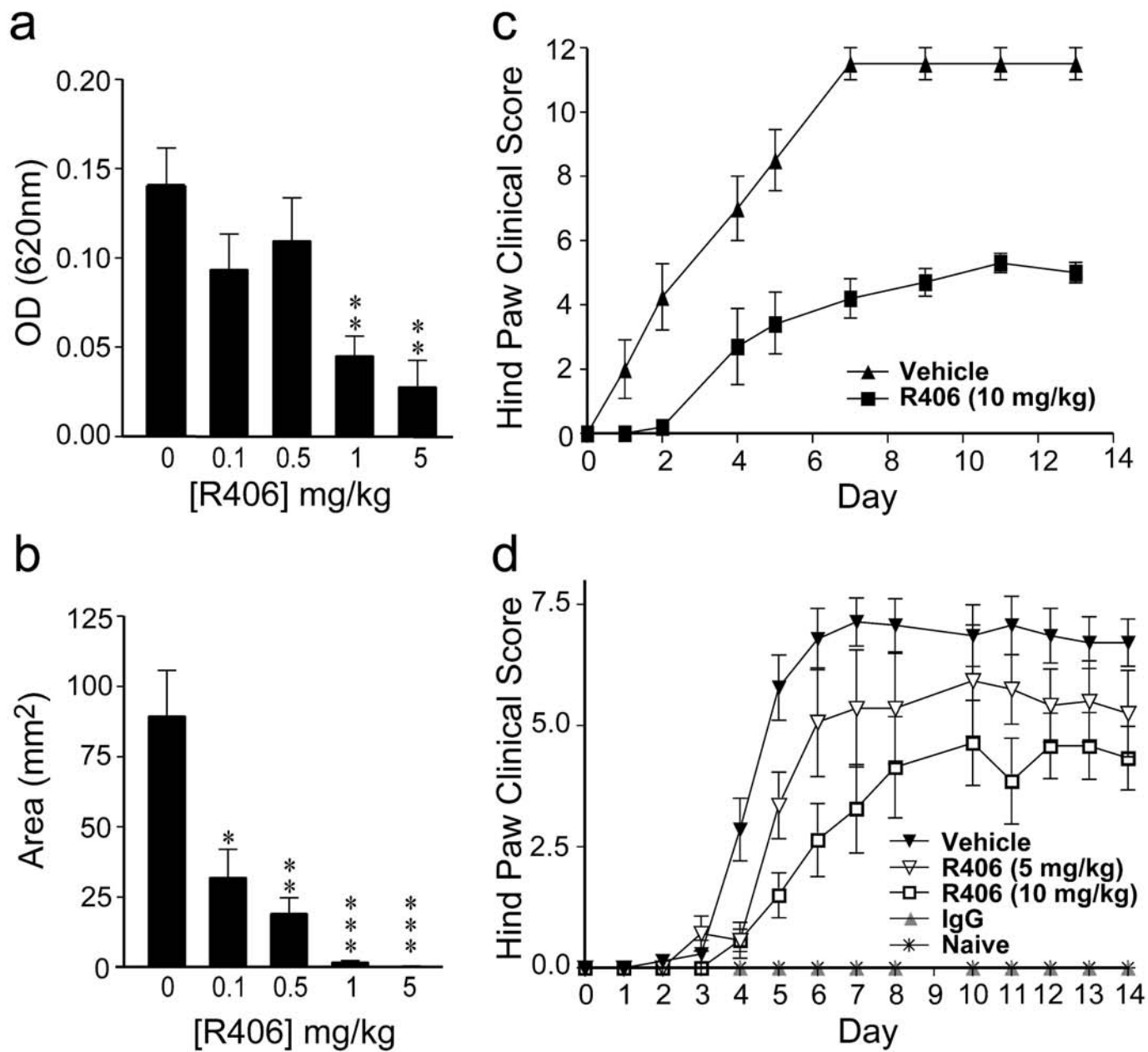Abbreviation: ICW, In Cell Western

Figure 1
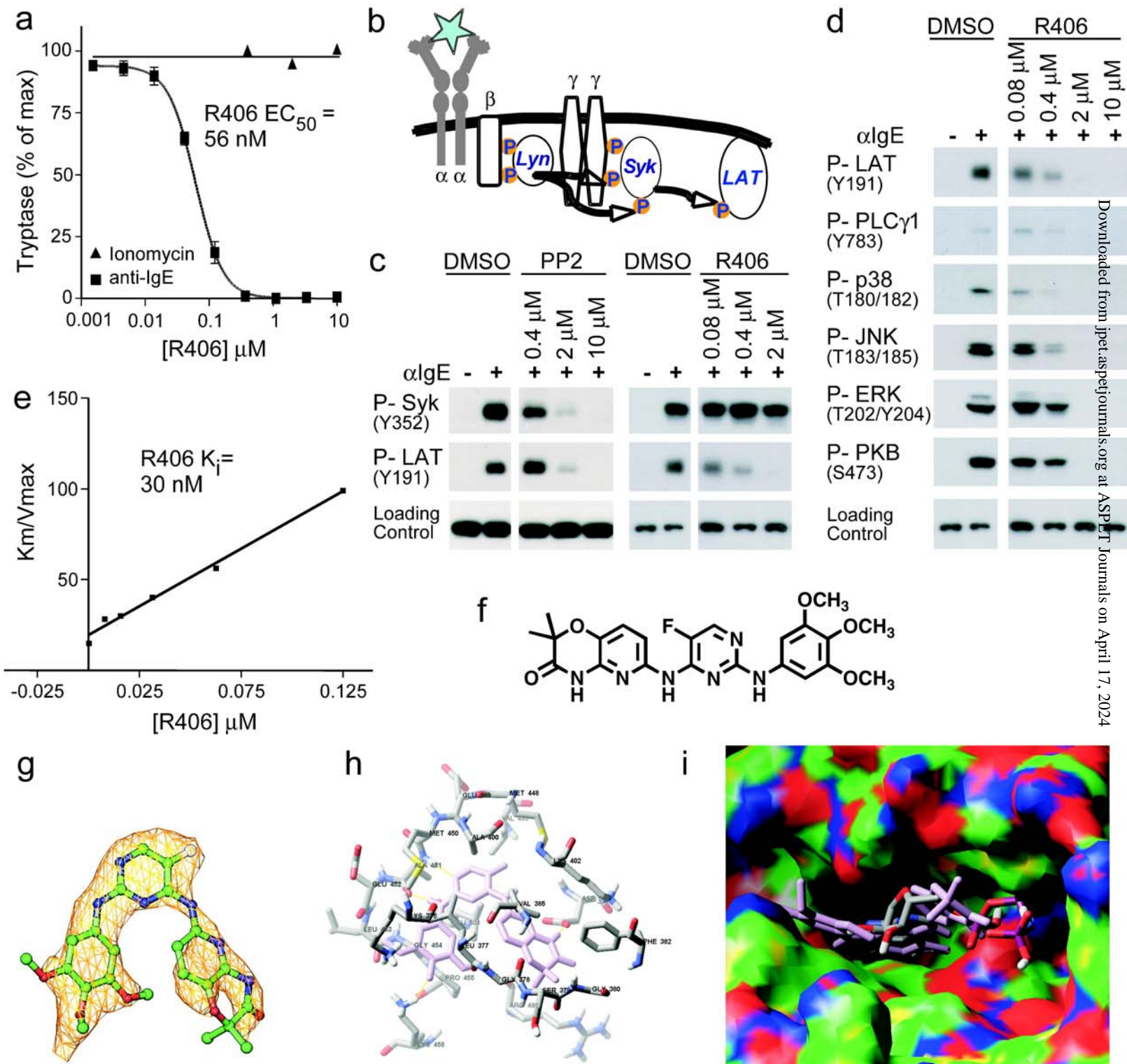
Figure 2

Figure 3

Figure 4

Figure 5